Radio Observations of the Magnetic Fields in Galaxies

M. Krause

(*Max-Planck-Institut für Radioastronomie, Auf dem Hügel 68, D-53121 Bonn, Germany*)

Abstract After a short introduction on how we get information of the magnetic fields from radio observations I discuss the results concerning the magnetic field structure in galaxies: Large-scale regular magnetic field pattern of spiral structure exists in grand-design spirals, flocculent and even irregular galaxies. The regular field in spirals is aligned along the optical spiral arms but strongest in the interarm region, sometimes forming 'magnetic arms'. The strongest total field is found in the optical arms, but mainly irregular. The large-scale regular field is best explained by some kind of dynamo action. Only a few galaxies show a dominant axisymmetric field pattern, most field structures seem to be a superposition of different dynamo modes or rather reveal more local effects related to density waves, bars or shocks. Observations of edge-on galaxies show that the magnetic fields are mainly parallel to the disk except in some galaxies with strong star formation and strong galactic winds as e.g. NGC 4631.

1 Introduction or What do we get from Radio Observations?

Radio observations of the continuum emission are best suitable to study the magnetic fields in galaxies. The total intensity of the synchrotron emission gives the strength of the total magnetic field. The linearly polarized intensity reveals the strength and the structure of the resolved regular field in the plane of the sky. However, the observed polarization vectors suffer Faraday rotation and depolarization (i.e. a decrease of the degree of linear polarization when compared to the intrinsic one) on the way from the radiation's origin to us. Correction for Faraday rotation is possible with observations at two or better more wavelengths by determining the rotation measure RM (being proportional to $\int n_{\rm e} B_{\parallel} dl$). The rotation measure itself is a measure of the magnetic field strength parallel to the line of sight, whereas its sign gives the direction of this magnetic field component. The field strength of both components, parallel and perpendicular to the line of sight, together with the information of the intrinsic polarization vectors enables us in principle to perform a 'tomography' of the magnetic field.

2 Faraday Rotation and Depolarization Effects

Figure 1 gives an example of observations of M51 at 4 different wavelengths, all smoothed to the same linear resolution of 75″ HPBW. The vectors are rotated by 90 deg but not corrected for Faraday rotation. The figure illustrates nicely the different effects of Faraday rotation and depolarization effects depending on the observing wavelength: the observed vectors at $\lambda 2.8$ cm and $\lambda 6$ cm are mainly parallel to the optical spiral arms as expected in spiral galaxies (see below), Faraday rotation is small at centimeter wavelengths. However, the pattern looks very different at $\lambda 18/20$ cm where Faraday rotation is expected to be strong. Further, we see a region in the northeastern part of M51 with complete depolarization.

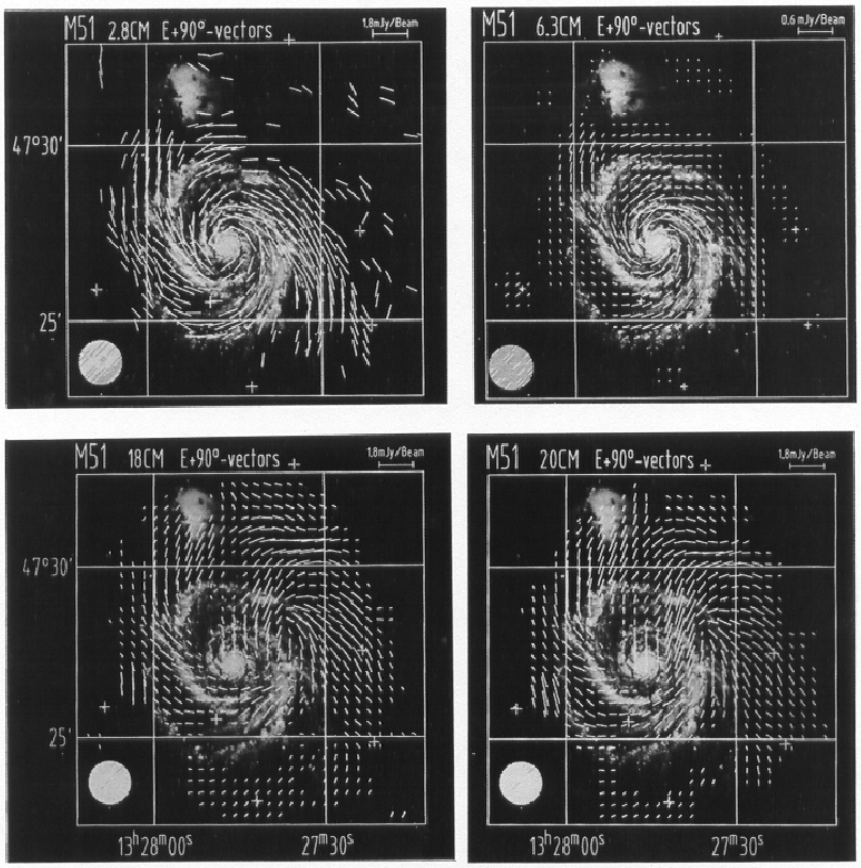

Fig. 1 Maps of the E-vectors rotated by 90° of M51 observed at $\lambda\lambda$2.8 cm, 6.2 cm, 18.0 cm, and 20.5 cm. The length of the vectors is proportional to the polarized intensity. They are shown superimposed onto an optical picture (Lick Observatory).

After substraction of the thermal fraction of the emission we distinguish between beam-dependent and wavelength-dependent depolarization. The difference in depolarization at different wavelengths in maps with the same linear resolution should be purely wavelength dependent where two different wavelength-dependent depolarization effects are important to consider: the differential Faraday rotation and Faraday dispersion as despcribed by Burn (1966) and Sokoloff et al. (1998). The latter effect is due to turbulent magnetic fields within the source and between the source and us, whereas the Faraday rotation depends on the regular magnetic field within the emitting source. The differential Faraday rotation has a strong wavelength dependence as shown e.g. in Fig. 1 in Sokoloff et al. (1998) leading to a complete depolarization at λ20 cm already at a RM $\approx 40\,\mathrm{rad/m^2}$, with again decreasing depolarization for higher RMs. Such an effect has first been detected in small isolated areas in M51 (Horellou et al. 1992). At λ6 cm the depolarization is much smaller, increasing smoothly to zero at RM $\approx 400\,\mathrm{rad/m^2}$ (the first zero point is at RM $= \pi/(2 \cdot \lambda^2)$).

Hence, the galaxies may not be transparent in linear polarization at decimeter wavelengths so that we may observe just an upper layer of the whole disk. At centimeter wavelengths we do not expect complete depolarization even in galaxies viewed edge-on, i.e. cen-

timeter wavelengths are best suitable to trace the magnetic field structure.

3 Magnetic Field Strength and Structure

The total magnetic field strength in a galaxy can be estimated from the nonthermal radio emission under the assumption of equipartition between the energies of the magnetic field and the relativistic particles (the so called **energy equipartition**). The degree of linear polarization and some assumptions of the geometry of the magnetic field give the strength of the magnetic field that has a uniform direction within the beam size. The estimates are based on the formulae given by e.g. Pacholczyk (1970) and Segalowitz et al. (1976), and are described e.g. by Krause et al. (1984) and Beck (1991).

3.1 Magnetic Fields in Spiral Galaxies

The magnetic field has been found to be mainly parallel to the galactic disk and to show a large spiral pattern similar to that of the optical spiral arms. The total magnetic field strength is generally highest at the positions of the optical spiral arms, whereas the highest regular fields are found *offset* of the optical arms and in the interarm region.

The mean equipartition value for the total magnetic field strength for a sample of 74 spiral galaxies observed by Niklas (1995) is on average $8\,\mu$G with a standard deviation of $3\,\mu$G. It can however reach values of about $20\,\mu$G *within* spiral arm regions as e.g. in NGC 6946 (Beck 1991). Strongly interacting galaxies or galaxies with a strong central radio emission tend to have generally stronger total magnetic fields. The strengths of the *regular* fields are typically 1-5 μG in the *interarm* regions in nearby spirals but reach locally $13\,\mu$G in NGC 6946 (Beck & Hoernes 1996).

3.2 Regular Magnetic Fields and Dynamo Action

The large-scale magnetic field is generally thought to be amplified and maintained by the action of a large-scale dynamo. According the mean field dynamo theory (e.g. Ruzmaikin et al. 1988; Wielebinski & F. Krause 1993; Beck et al. 1996; Lesch & Chiba 1997) the structure of the large-scale field is also given by the dynamo action. It is generally of spiral shape with different azimuthal field directions and symmetries. The mode that can be excited most easily is the axisymmetric mode (**ASS**) followed by higher modes as the bisymmetric (**BSS**), etc. The field configurations can be either symmetric (quadrupole type) or asymmetric (dipole type) with respect to the galactic plane. According to the dynamo theory the pitch angle of the magnetic field spiral is determined by the dynamo numbers, not by the pitch angle of the gaseous spiral arms.

The ASS and BSS field configurations can be distinguished observationally by analyzing the rotation measures or – more sophisticated – by analyzing directly the observed polarization vectors at different wavelengths (as has been described e.g. in Sokoloff et al. (1992) and Berkhuijsen et al. (1997)). It has been found that only M31 and IC342 show clear ASS fields (Beck 1982; Krause et al. 1989a), whereas many other galaxies seem to have a superposition of different modes.

A special case is M81 as it has a *dominating* BSS field field (Krause et al. 1998b; Sokoloff et al. 1992). The dominance of the BSS field structure requires additional physical mechanism to be invoked that can occur only in rare cases. For M81 a three-dimensional, nonlinear dynamo model has been developed including the disturbed velocity field due to the encounter with its companion NGC 3077 (Moss et al. 1993) or alternatively, parametric resonance with the spiral density wave as has been proposed by Chiba & Tosa (1990) and

investigated numerically by Moss (1996).

Most other spiral galaxies observed so far indicate a mixture of magnetic modes. The analysis of the observations at all 4 frequencies of M51 (Fig. 1) revealed even two different magnetic field configurations for the disk and the halo resp. (Berkhuijsen et al. 1997): a halo with an axisymmetric field configuration parallel to the disk with magnetic field lines pointing *inwards* and a superposition of an axisymmetric and a bisymmetric field with about equal weights in the disk. The magnetic field lines in the disk are spirals generally directed *outwards* except in a few sectors in the inner northwestern part of M51 as shown in Fig. 2.

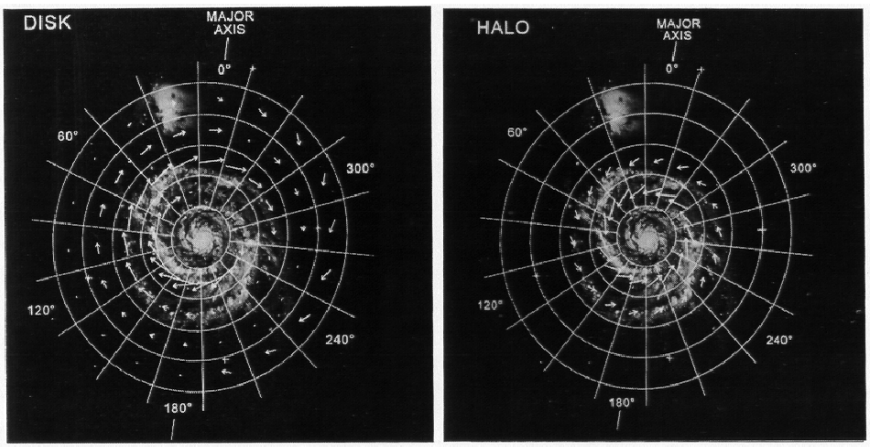

Fig. 2 The vectors give the directions of the horizontal regular magnetic field in the disk (left) and the halo (right) of M51 as fitted to the observations at 4 different wavelengths in Fig. 1. They are shown superimposed onto an optical picture (Lick Observatory). Note that the magnetic field direction in the disk is opposite to that in the halo, except in a few sectors in the inner northwestern part of the galaxy.

It is clear that such a global description of the regular magnetic field cannot describe local effects that become more and more visible with increasing linear resolution of the observations. Further, in grand-design galaxies the magnetic field lines follow quite often the dust lanes. In M51 e.g. one dust lane in the eastern part crosses the optical spiral arm, so does the regular magnetic field (visible in Fig. 1 at in the short wavelengths observations).

3.3 Magnetic Arms

The regular interarm field in M81 fills the whole interarm region. Different to this some galaxies host so-called *magnetic arms*. Long, highly polarized arms disconnected from the optical spiral arms were first discovered in IC342 (Krause et al. 1989a; Krause 1993). Two symmetric magnetic arms running right in the interarm region parallel to the optical spiral arms were found in NGC 6946. Their width is less than 1 kpc, hence they do not fill the whole interarm region. Magnetic arms have also been found in NGC 2997 (Han et al. 1999) and M83 (Beck, Ehle & Sukumar in prep.).

Several models have been developed to explain these magnetic arms. Slow MHD waves have been proposed by Fan & Lou (1996) and Lou & Fan (1998) to explain the generation of magnetic arms shifted with respect to the optical spiral arms. These MHD waves occur only in an almost rigidly rotating disk. However, all galaxies with magnetic arms are found to rotate differentially beyond 1—2 kpc from the center, different to older measurements with lower angular resolution. Han et al. (1999) found some correlation between the magnetic arms and interarm gas features generated at the 4:1 resonances in numerical models of Patsis

et al. (1997).

In the framework of dynamo theory the generation of magnetic arms can be described if one considers that the turbulent velocity of the gas is higher in the optical arms (Moss 1998; Shukurov 1998), or that turbulent diffusion is larger in the arms (Rohde et al. 1999). Both effects reduce the dynamo number in the spiral arms when compared to the interarm regions and hence allow to generate magnetic arms preferently in the interarm region.

3.4 Magnetic Fields in Flocculent and Irregular Galaxies

Regular magnetic fields have also been detected in flocculent galaxies like M33 (Buczilowski & Beck 1991) and NGC 4414 (Soida et al. 2002). These are galaxies with a flocculent spiral structure without signs of the action of density waves. The mean degree of polarization (corrected for different angular resolution) is similar between flocculent and grand-design galaxies (Knapik et al. 2000). As expected from classical $\alpha - \Omega$ dynamo models the dynamo works well without the assistance of density waves.

Even in a dwarf irregular galaxy with weak rotation and non-systematic gas motion like NGC 4449 a large-scale (partly spiral) regular magnetic field has been observed (Chyzy et al. 2000). The strength of the regular field reaches $7\,\mu$G and that of the total field $14\,\mu$G, which is high even in comparison with fields strengths of radio-bright spirals. The absence of ordered differential rotation requires a different kind of dynamo action in this galaxy. A fast field amplification is predicted by a dynamo e.g. driven by magnetic buoyancy and sheared Parker instabilities (e.g. Moss et al. 1999; Hanasz & Lesch 1998, 2000) or without any α effect at all (Blackman 1998).

3.5 The magnetic fields in Barred Galaxies and Other Shocked Areas

A sample of 20 barred galaxies has been observed extensively in total power and linear polarization (Beck et al. 2002). They found that the total radio emission (and hence the total magnetic field) is strongest along the bar and correlates with the bar *length*. The regular magnetic field is enhanced *upstream* of the shock fronts in the bar. The upstream field lines are at large angle to the bar, but turn sharply towards the bar about 1 kpc upstream from the dust lanes as observed in NGC 1097 (Beck et al. 1999). According to these authors similar effects have also been observed in NGC 1365, NGC 1672, and NGC 7552.

Indications for a compression of the galactic magnetic field possibly by gas tidally stripped during an interaction with the neighbouring galaxy have been observed in NGC 3627 (Soida et al. 2001) where the observed regular field apparently crosses the dust lanes at a large angle in the east. Another example for such a compression is the wind-swept galaxy NGC 4254 (Soida et al. 1996).

3.6 Edge-on Galaxies and Vertical Fields

Several galaxies seen edge-on have been observed in radio continuum and polarization. Most of them have regular magnetic fields that are parallel to the galactic disks (Dumke et al. 1995), only a few are found with large-scale vertical fields like M82 (Reuter et al. 1994), NGC 4631 (Golla & Hummel 1994), NGC 4666 (Dahlem et al. 1997), and NGC 5775 (Tüllmann et al. 2000).

The apparent disk thicknesses vary quite a lot among the galaxies with plane-parallel field as well as their intensities does. Interferometer observations of edge-on galaxies have to be combined with single-dish observations in order to correct for the missing zero-spacings before the scale heights of the emission perpendicular to the disk (in z-direction) can be determined. We found that the emission in z-direction can best be fitted with two exponential functions, whose scale heights are about *equal* for all four galaxies with plane-parallel fields

that have been analyzed so far, namely NGC 891, NGC 3628, NGC 4565, NGC 5907 (Dumke & Krause 1998; Dumke et al. 2000). The scale height for the thin disk is $\simeq$ 300 pc and that of the thick disk/halo is $\simeq$ 1.8 kpc for these galaxies, independent of the star-forming activity and interaction state.

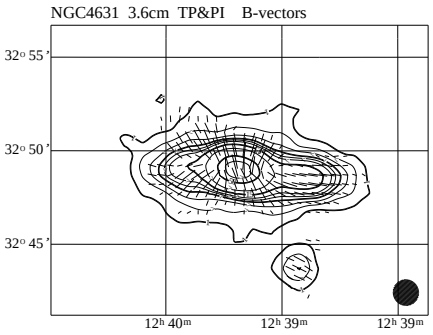

Fig. 3 Contour map of NGC 4631 at λ3.6 cm as observed with the Effelsberg 100 m telescope. The angular resolution is 85″ HPBW. The vectors give the orientation of the intrinsic regular field in the plane of the sky. Their lengths are proportional to the polarized intensity.

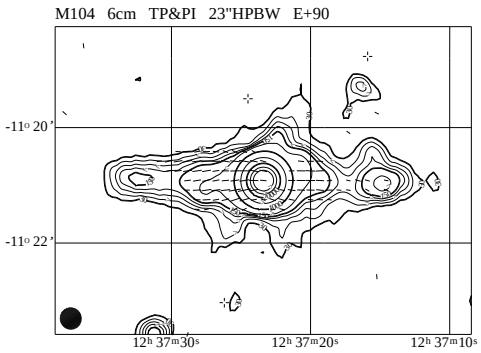

Fig. 4 Contour map of M104 at λ6.2 cm as observed with the VLA in D array. The angular resolution is 23″ HPBW. The vectors give the observed E-vectors rotated by 90° , their lengths are proportional to the polarized intensity.

Recent λ3.6 cm observations of NGC 4631 obtained with the Effelsberg 100 m telescope are presented in Fig. 3. Faraday rotation could be determined between this wavelength and λ6.2 cm observations with the VLA and revealed $-300\,\mathrm{rad/m^2} < \mathrm{RM} < 300\,\mathrm{rad/m^2}$. The vectors shown in Fig. 3 give the intrinsic magnetic field orientation. NGC 4631 has a large-scale vertical magnetic field in the central 7 kpc. Outside this radius the field is plane parallel in the western half but still has vertical field components in the eastern half. The RM does not show a typical symmetric pattern as expected from a dipole or quadrupole field. Hence we conclude that the vertical field is rather wind-driven and related to the high star-forming activity in this galaxy. The exponential scale heights for NGC 4631 are about 50% larger than those found for galaxies with plane-parallel fields which may also be related to the galactic winds and vertical fields.

Another edge-on galaxy is M104, the Sombrero galaxy, classified as an Sa galaxy and known for its huge bulge. We observed M104 at λ6.2 cm with the VLA in D array and detected that the observed E+90° vectors are surprisingly regular and mainly parallel to the galactic disk as shown in Fig. 4. Unfortunately, the observations could not yet be corrected for Faraday rotation because we have no observations at another wavelength. The regularity of the vectors at λ6.2 cm may indicate that Faraday rotation is rather small. Hence it seems that the regular magnetic field in M104 is mainly disk parallel, also inside the central 6 kpc where the rotation curve is still rising. The radio emission in z-direction can best be fitted by a one-component Gaussian rather than an exponential function with a scale height of $\simeq$ 3 kpc. According to Combes (1991) a Gaussian z-distribution is just expected for a thin disk inside a self-gravitating mass distribution, i.e. the huge bulge in M104.

References

Beck R., A&A, 1982, 106, 121
Beck R., A&A, 1991, 251, 15
Beck R., Hoernes P., Nature, 1996, 379, 47
Beck R., Brandenburg A., Moss D., et al., ARA&A, 1996, 34, 155
Beck R., Ehle M., Shoutenkov V., et al., Nature, 1999, 397, 324
Beck R., Shoutenkov V., Ehle M., et al., A&A, 2002, 391 83
Berkhuijsen E.M., Horellou C., Krause M., et al., A&A, 1997, 318, 700
Blackman E.G., ApJ, 1998, 496, L17
Buczilowski U.R., Beck R., A&A, 1991, 241, 47
Burn B.J. MNRAS, 1966, 133, 67
Chiba M., Tosa M., MNRAS, 1990, 244, 714
Chyzy K.T., BeckR., Kohle S., et al., A&A, 2000, 355, 128
Combes F., ARA&A, 1991, 29, 195
Dahlem M., Petr M.G., Lehnert M.D., et al., A&A, 1997, 320, 731
Dumke M., Krause M., Wielebinski R., et al., A&A, 1995, 302, 691
Dumke M., Krause M., IAU Coll. 166, The Local Bubble and Beyond, In: Breitschwerdt D., Freyberg M., eds., Lecture Notes in Physics 506, Springer Verlag, Berlin, 1998, 555
Dumke M., Krause M., A&A, 2000, 355, 512
Fan Z., Lou Y.Q., Nature, 1996, 383, 800
Golla G., Hummel E., A&A, 1994, 284, 777
Han J.L., Beck R., Ehle M., et al., A&A, 1999, 348, 40
Hanasz M., Lesch H., A&A, 1998, 332, 77
Hanasz M., Lesch H., ApJ, 2000, 543, 235
Horellou C., Beck R., Berkhuijsen E.M., et al., A&A, 1992, 265, 417
Knapik J., Soida M., Dettmar R.J., et al., A&A, 2000, 362, 910
Krause M., IAU Symp. 140, Galactic and Intergalactic Magnetic Fields, In: Beck R., Kronberg P.P., Wielebinski R., eds., Kluwer, Dordrecht, 1990, 187
Krause M., IAU Symp. 157, The Cosmic Dynamo, Krause F., et al., ed., Kluwer, Dordrecht, 1993, 305
Krause M., Beck R., Klein U., A&A, 1984, 138, 385
Krause M., Hummel E., Beck R., A&A, 1989a, 217, 4
Krause M., Beck R., Hummel E., A&A, 1989b, 217, 17
Lesch H., Chiba M., Fund. Cosmic Phys., 1997, 18, 273
Lou Y.Q., Fan Z., ApJ, 1998, 493, 102
Moss D., A&A, 1996, 308, 381
Moss D., MNRAS, 1998, 297, 860
Moss D., Brandenburg A., Donner K.J., et al., ApJ, 1993, 409, 179
Moss D., Shukurov A., Sokoloff D., A&A, 1999, 343, 120
Niklas S., PhD thesis, University of Bonn, 1995
Pacholczyk A.G., Radio Astrophysics, Freeman, San Francisco, 1970
Patsis P.A., Grosbøl P., Hiotelis N., A&A, 1997, 323, 762
Reuter H.P., Klein U., Lesch H., et al., A&A, 1994, 282, 724
Rohde R., Beck R., Elstner D., A&A, 1999, 350, 423
Ruzmaikin A.A., Shukurov A.M., Sokoloff D.D., Magnetic Fields of Galaxies, Kluwer, Dordrecht, 1988
Segalovitz A., Shane W.W., de Bruyn A.G. Nature, 1976, 264, 222
Shukurov A., MNRAS, 1998, 299, L21
Soida M., Urbanik M., Beck, R. A&A, 1996, 312, 409
Soida M., Urbanik M., Beck R., et al., A&A, 2001, 378, 40
Soida M., Beck R., Urbanik M., et al., A&A, 2002, 394, 47
Sokoloff D., Shukurov A., Krause M., A&A, 1992, 264, 396
Sokoloff D.D., Bykov A.A., Shukurov A., et al., MNRAS, 1998, 299, 189
Tüllmann R., Dettmar R.-J., Soida M., et al., A&A, 2000, 364, L36
Wielebinski R., Krause F., A&AR, 1993, 4, 449